AtTMEM18 plays important roles in pollen tube and vegetative growth in Arabidopsis

Xiao-Ying Dou[1,2], Ke-Zhen Yang[2], Zhao-Xia Ma[2], Li-Qun Chen[2], Xue-Qin Zhang[2], Jin-Rong Bai[1] and De Ye[2]*

[1]Beijing Radiation Center, 12 Haidian Nanlu, Beijing 100875, China, [2]State Key Laboratory of Plant Physiology and Biochemistry, College of Biological Sciences, China Agricultural University, 2 Yuanmingyuan Xilu, Beijing 100193, China. *Correspondence: yede@cau.edu.cn

Abstract In flowering plants, pollen tube growth is essential for delivery of male gametes into the female gametophyte or embryo sac for double fertilization. Although many genes have been identified as being involved in the process, the molecular mechanisms of pollen tube growth remains poorly understood. In this study, we identified that the *Arabidopsis Transmembrane Protein 18* (*AtTMEM18*) gene played important roles in pollen tube growth. The AtTMEM18 shares a high similarity with the Transmembrane 18 proteins (TMEM18s) that are conserved in most eukaryotes and may play important roles in obesity in humans. Mutation in the *AtTMEM18* by a *Ds* insertion caused abnormal callose deposition in the pollen grains and had a significant impact on pollen germination and pollen tube growth. *AtTMEM18* is expressed in pollen grains, pollen tubes, root tips and other vegetative tissues. The pollen-rescued assays showed that the mutation in *AtTMEM18* also caused defects in roots, stems, leaves and transmitting tracts. AtTMEM18-GFP was located around the nuclei. Genetic assays demonstrated that the localization of AtTMEM18 around the nuclei in the generative cells of pollen grains was essential for the male fertility. Furthermore, expression of the rice TMEM18-homologous protein (OsTMEM18) driven by *LAT52* promoter could recover the fertility of the *Arabidopsis attmem18* mutant. These results suggested that the TMEM18 is important for plant growth in *Arabidopsis*.

INTRODUCTION

In higher plants, pollen tube elongation in the pistil is a crucial step for sexual reproduction (Xia et al. 2010). The process begins with deposition of pollen grains on the stigmatic tissue. The compatible interaction between pollen and stigmatic cells triggers the hydration and germination of the pollen grains (Jiang et al. 2005). The resulting pollen tube invades the stigmatic tissue, penetrates the style, navigates through the transmitting tract, and then is guided toward the ovule to deliver the sperm cells into the embryo sac for fertilization (Hülskamp et al. 1995; Wilhelmi and Preuss 1996; Ray et al. 1997; Lennon and Lord 2000; Palanivelu and Preuss 2000; Johnson and Preuss 2002; Lord and Russell 2002; Preuss 2002; Kim et al. 2003; Palanivelu et al. 2003).

Pollen tube elongation is a polar growth event, namely the growth exclusively occurs at the tip (Bedinger 1992; Krichevsky et al. 2007; Chebli et al. 2012). Many cell biological processes are involved in pollen tube growth, such as calcium gradients (Iwano et al. 2009), vesicular trafficking (Šamaj et al. 2006), actin cytoskeleton dynamics (Wilsen et al. 2006), ion fluxes (Michard et al. 2009), energy metabolism (Hepler et al. 2013) and cell wall synthesis (Chebli et al. 2012; Guan et al. 2013).

Cell wall plays a crucial role in maintaining cell integrity under high turgor pressure (Chebli et al. 2012; Guan et al. 2013).

Cell wall synthesis mainly occurs in the tip region of growing pollen tubes. The newly formed cell wall at the pollen tube tip is mainly composed of pectins (Lancelle and Hepler 1992; Edlund et al. 2004; Geitmann and Steer 2006; Dardelle et al. 2010; Chebli et al. 2012), which are synthesized in the Golgi apparatus and secreted by exocytosis, and are highly methyl-esterified. In the subapical and distal region of the pollen tubes, the pectins are de-esterified by pectin methylesterase (PME) to confer the rigidity (Jiang et al. 2005; Harholt et al. 2010). Behind the tip of the pollen tube, a secondary layer is formed beneath the outer pectic layer (Ferguson et al. 1998; Li et al. 1999a). The most abundant component in this secondary wall layer is callose. Cellulose is also present in this layer, but at a low level (Dong et al. 2005; Nishikawa et al. 2005; Geitmann and Steer 2006). Callose deposition was first detected immediately after germination of pollen grains in liquid medium, at the rim of the germination aperture (Li et al. 1999b). In pollen tube, callose can be steadily detected in the distal region, which is confined to the inner wall layer and to transverse walls named plugs (Ferguson et al. 1998; Li et al. 1999b). The plugs were consistent with its role in resisting tension stresses (Chebli et al. 2012). However, how the genes regulate the callose deposition in pollen tube remains poorly understood.

The tip growth events of cells include pollen tube and root hair growth in higher plants, nerve growth and axon guidance in animals, and hyphal growth in fungi (Li et al. 1999b). Many genes have been identified as being involved in tip growth, including the *Transmembrane protein 18* (*TMEM18*) in animals. The TMEM18 is predicted to consist of α helices and has three transmembrane domains (Speakman 2013). Phylogenetic analysis has revealed that TMEM18 has an ancient origin, being found in plants and most other eukaryotic organisms (Almén et al. 2010; Speakman 2013). TMEM18 is located in the nuclear envelope in neural stem cells (Jurvansuu et al. 2008) and has been proposed to be involved in cell migration as demonstrated by overexpression of the protein increasing the migration of neural stem cells towards glioma in the rat brain (Jurvansuu et al. 2008). The TMEM18 is expressed ubiquitously with differences in expression levels in the different tissues (Speakman 2013). In mouse brain, its highest expression occurred in the hypothalamus, thalamus and substantia nigra. The hypothalamus is the region that is responsible for the control of energy homeostasis. Recently TMEM18 was identified to be involved in obesity and body mass index (BMI) (Almén et al. 2010). Nevertheless, so far, little is known about the function of TMEM18. Especially, the roles and functions of the TMEME18 protein in plant species remain unknown.

In this study, the *Arabidopsis thaliana TMEM18* (*AtTMEM18*) was identified by a screening for male gametophyte-defective mutant from the gene- and enhancer-trap *Ds* insertional mutant library (Sundaresan et al. 1995; Yang et al. 1999). AtTMEM18 is encoded by *At1g34350* and shares a higher similarity with the TMEM18 proteins from other species. The insertion of the *Ds* in *At1g34350* caused an unusual deposition of callose in the germinating pollen grains and affected the growth of pollen tubes and vegetative organs, indicating that AtTMEM18 plays important roles in the pollen tube and cell morphogenesis.

RESULTS

Isolation and genetic analysis of the *attmem18* mutant

The *attmem18* mutant was isolated in a genetic screen for male gametophyte-defective mutants from a collection of gene-trap and enhancer-trap *Ds* insertion lines in *Arabidopsis* ecotype Landsberg *erecta* (L*er*) (Sundaresan et al. 1995). The *Ds* insertion created a genetic tag of kanamycin resistance in the mutant plant. At first, a genetic analysis of the heterozygous *attmem18-1* (*attmem18*/+) plants was performed (Table 1). The progeny from self-pollinated *attmem18*/+ plants exhibited a segregation ratio of approximately 1 kanamycin-resistant

(Kan^R): 1 kanamycin-sensitive (Kan^S) (1282:1278), much lower than the typical Mendelian segregation ratio of 3 to 1. Furthermore, no homozygous Kan^R plants (*attmem18*/-) were identified in the progeny. This result indicates that the *attmem18* mutant is defective in gametophytic function.

To determine how the mutation affected male or female gametophytic functions, the *attmem18*/+ plants were used as males or females to cross with wild type plants. As shown in Table 1, when the *attmem18*/+ plants were used as female parents, 50.71% (710/1400) of the resulting F1 progeny were Kan^R. In contrast, when *attmem18*/+ pollen grains were used to pollinate wild type plants, no Kan^R plants in the F1 progeny were obtained (0:2237). Thus, the *attmem18* mutation disrupted male gametophytic function completely, but did not affect female gametophytic function.

The *attmem18* pollen grains exhibited an abnormal callose deposition

To investigate how *attmem18* affected male gametophytic function, observation of *attmem18* male gametophyte development was performed. Scanning electron microscopy (SEM) showed that most of the pollen grains from the *attmem18*/+ plants were as normal as wild type pollen grains in morphology (Figure 1A, B). 4′6-diamidino-2-phenylindole (DAPI) staining showed that the pollen grains from the *attmem18*/+ plants had two sperm nuclei and a vegetative nucleus like wild type pollen grains (Figure 1C, D). These results indicated that the *attmem18* mutation did not affected pollen formation.

Aniline blue, which is a specific dye for callose, was used to study the callose deposition pattern in the *attmem18* pollen by comparison with wild type pollen. No obvious fluorescence signal was observed in wild type pollen grains (Figure 1E) as expected. In contrast, 23.2% of pollen grains from *attmem18*/+ plants exhibited the dotted fluorescence signals (Table S1, Figure 1F), indicating that a number of *attmem18*/+ pollen grains had an abnormal callose deposition. Because no homozygous *attmem18* mutant could be generated for the assays, *attmem18* mutant was introgressed into a background of *quartet1-2* (*qrt1-2*) mutant to perform quartet assay (Preuss et al. 1994). The *qrt1-2* mutation blocks physical separation of the tetrad pollen grains, but does not affect the germination and growth of the pollen tubes (Preuss et al. 1994). Therefore, a tetrad from the *attmem18*/+; *qrt1/qrt1* mutant plants had two *qrt1-2* (presenting wild type) pollen gains and two *qrt1-2*; *attmem18* (presenting *attmem18* mutant) pollen grains. When the tetrads pollen grains from *qrt1-2* and *attmem18*/+; *qrt1/qrt1* plants were stained with aniline blue, no obvious fluorescence could be seen in *qrt1-2* pollen grains from the *qrt1/qrt1* mutant plant, while 24.1% of pollen grains from the *attmem18*/+; *qrt1-2/ qrt1-2* plants showed dotted callose deposition patterns (Table S1, Figure 1G, H), indicating that the pollen grains carrying the *attmem18* in the tetrads exhibited an unusual callose deposition.

To verify the location of callose deposition in the *attmem18* pollen grains, callose-specific antibody was used to locate the callose in the section of *attmem18* pollen grains from the *attmem18*/+ plants. As shown in Figure 1J, the punctate callose signals appeared nearby the inner wall in the *attmem18* pollen grain sections, compared to that no obvious

Table 1. Genetic analysis of the *attmem18*/+ mutant

Crosses (Female × Male)	Number of Kan^R seedlings	Number of Kan^S seedlings	Kan^R/ Kan^S
attmem18/+ × *attmem18*/+	1,282	1,278	1.003
Wild type × *attmem18*/+	0	2,237	0
attmem18/+ × wild type	710	690	1.029

Kan^R, kanamycin-resistant; Kan^S, knanamycin-sensitive.
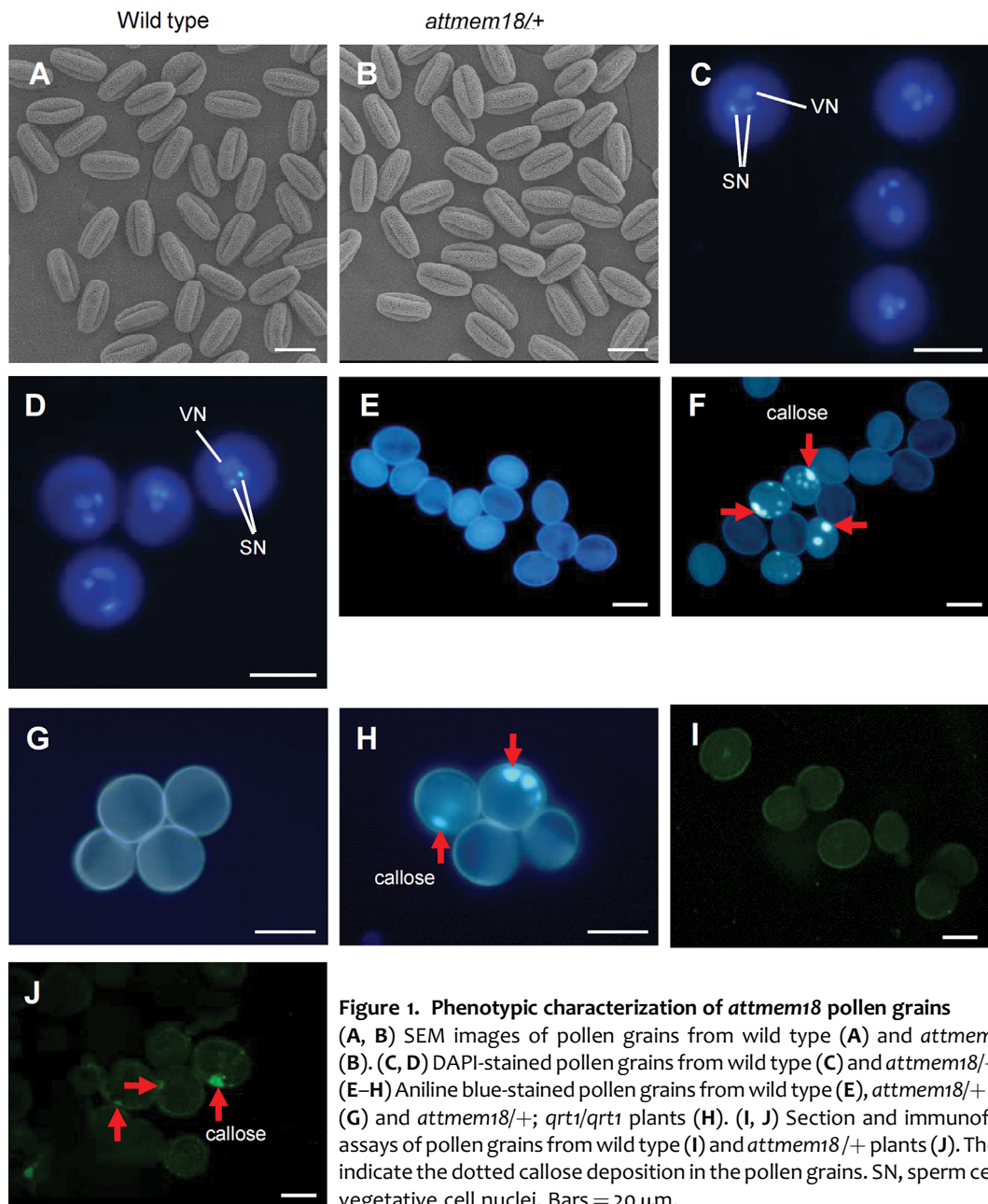
Wild type   attmem18/+

Figure 1. Phenotypic characterization of *attmem18* pollen grains
(**A, B**) SEM images of pollen grains from wild type (**A**) and *attmem18*/+ plants (**B**). (**C, D**) DAPI-stained pollen grains from wild type (**C**) and *attmem18*/+ plants (**D**). (**E–H**) Aniline blue-stained pollen grains from wild type (**E**), *attmem18*/+ (**F**), *qrt1/qrt1* (**G**) and *attmem18*/+; *qrt1/qrt1* plants (**H**). (**I, J**) Section and immunofluorescence assays of pollen grains from wild type (**I**) and *attmem18*/+ plants (**J**). The red arrows indicate the dotted callose deposition in the pollen grains. SN, sperm cell nuclei; VN, vegetative cell nuclei. Bars = 20 µm.

fluorescence signals were observed in the sections of the wild type pollen grains (Figure 1I). These results showed that the *attmem18* pollen grains had an abnormal callose deposition during germination process.

The *attmem18* pollen is defective in pollen germination and pollen tube growth

To study how *attmem18* mutation affected the male gametophytic function, we further examined the germination of *attmem18* pollen grains. The mature pollen grains from *attmem18*/+ plant were cultured *in vitro*. 39.8% of the pollen grains from *attmem18*/+ plants germinated *in vitro*, compared to that 76.2% of the pollen grains from wild type plants could germinate under the same culture condition (Figure 2A–C),

indicating that the *attmem18* significantly reduced pollen germination *in vitro*.

Then we examined the pollen germination efficiency of the *attmem18 in vivo*. After the pollen grains from *attmem18*/+ and wild type plants were pollinated to the emasculated wild type flowers for 12 h, they were observed by SEM, respectively. All the wild type pollen tubes could normally grow into the stigma (Figure 2D). In contrast, some of the pollen tubes generated by the pollen grains from *attmem18*/+ plants were short and swollen (Figure 2E). Among the pollen grains from *attmem18*/+ plants, 57.0% could grow morphologically normal pollen tubes, 18.4% did not germinate, and 24.6% produced shorter and swollen pollen tubes. In comparison, 95.9% of wild type pollen tubes could grow
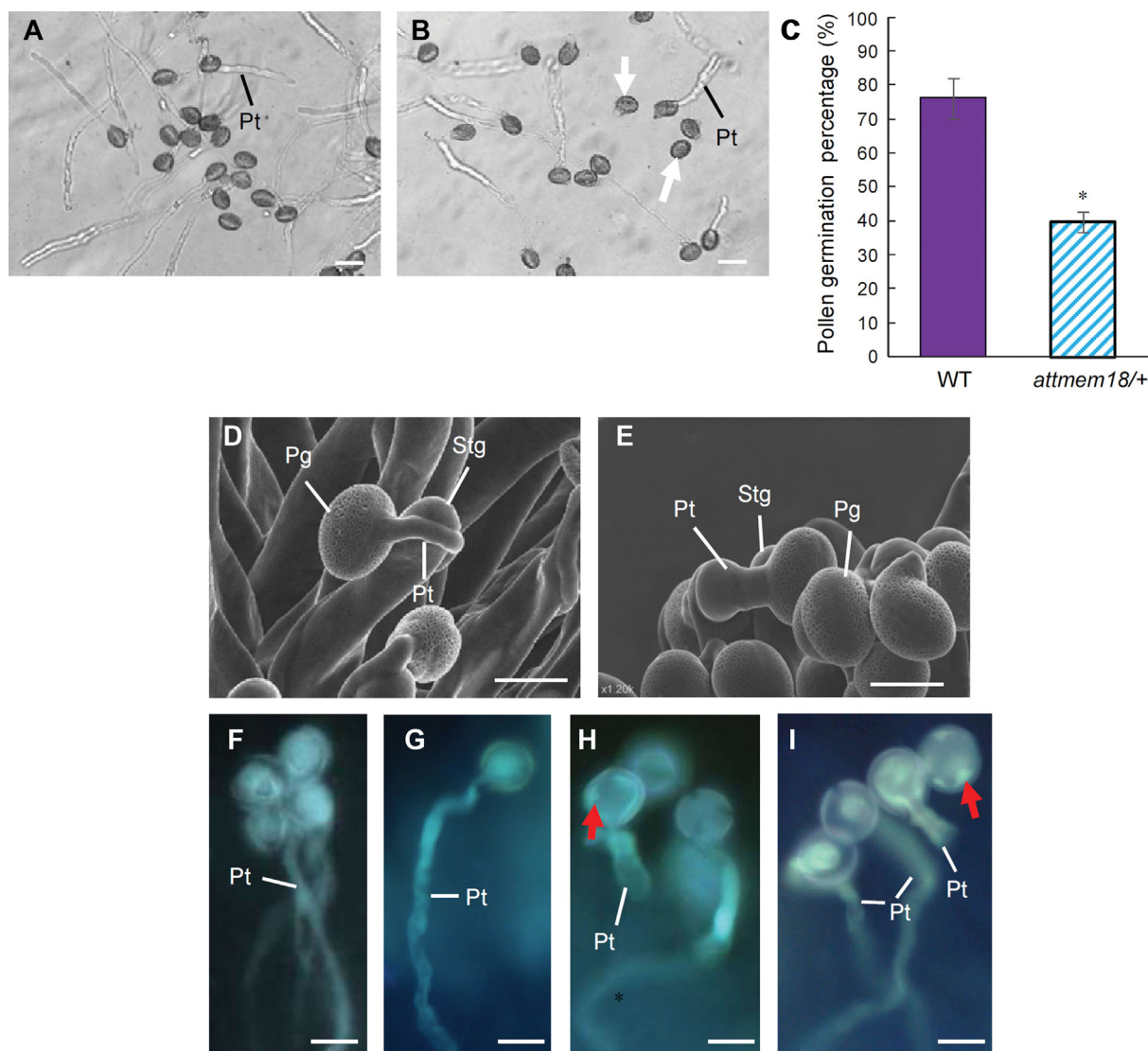
Figure 2. The *attmem18* affected *in vitro* and *in vivo* germination of pollen grains
(**A, B**) The *in vitro* germination of pollen grains from wild-type (**A**) and *attmem18*/+ plants (**B**). (**C**) Germination rates of pollen grains from wild type (WT) and *attmem18*/+ plants. (**D, E**) SEM images showing *in vivo* germination of the pollen grains from wild type (**C**) and *attmem18*/+ plants (**D**). (**F–I**) The *in vivo* germination of pollen grains from *qrt1/qrt1* plants (**F**), wild type (**G**), *attmem18*/+ (**H**) and *attmem18*/+; *qrt1/qrt1* plants (**I**). Pg, pollen grain; Pt, pollen tubes; Stg, stigmatic cells. White arrows indicate the ungerminated pollen grains. The red arrows indicate abnormal callose deposition in the pollen grains and pollen tubes. Bars = 20 μm. * $P < 0.05$.

normally through the stigma (Table S2). The quartet assays also achieved a similar result. In most tetrads from the *attmem18*/+; *qrt1/qrt1* plants, only 1 or 2 pollen grains could germinate pollen tubes. In general, 36.2% pollen grains produced normal pollen tubes, 35.0% pollen grains did not germinate, and 28.7% of pollen grains generated swollen pollen tubes (Table S2). In the control, most of the *qrt1-2* tetrads could have three or four pollen grains produce pollen tubes (Figure 2F). The germination rate was 68.1% (Table S2). Aniline blue staining showed that the callose deposition pattern in *attmem18* pollen tube inner walls was obviously different from that in wild type pollen tubes. In the

wild type, the callose exhibited as strong and round fluorescent signals, and uniformly distributed on the inner wall of pollen tubes. Callose plugs were formed in the elongating wild type pollen tubes (Figure 2G). In the *attmem18* mutant pollen grains from *attmem18*/+ and *attmem18*/+; *qrt1/qrt1* plants, callose exhibited as a punctate distribution pattern (Figure 2H, I) and distributed irregularly in the swollen pollen tube inner walls. The punctate distribution pattern was not found in the morphologically normal pollen tubes (Figure 2G, H). This result indicated that the abnormal callose deposition was likely related to the defect of the *attmem18* pollen tubes.

Phenotypes of *attmem18* could be complemented by wild type *AtTMEM18*

Thermal asymmetric interlaced PCR (TAIL-PCR) (Liu et al. 1995; Liu and Whittier 1995) was applied to obtain the flanking sequences adjacent to the *Ds* element in *attmem18*. Sequence analysis showed that the *Ds* element was inserted into the first exon of gene *At1g34350*, 261 bp downstream from start codon ATG (Figure 3A). The *Ds* insertion site was further confirmed by conventional PCR using the gene-specific (AtTMEM18-Ds-3′) and *Ds*-5′ border (Ds5-3) primers (Table S4).

To verify the phenotype of *attmem18*/+ was caused by the *Ds* insertion in *AtTMEM18* (*At1g34350*), the genomic sequence of *AtTMEM18*, which included the 1.0-kb promoter, 1.5-kb coding region and 3′-terminal region of *AtTMEM18*, was cloned into Ti-derived vector pCAMBIA1300 (CAMBIA, Australia) and introduced into the heterozygous *attmem18* (*attmem18*/+) plants via *Agrobacterium tumefaciens*-mediated infiltration transformation (Bechtold and Pelletier 1998). The seeds from the T1 transgenic *attmem18*/+ plants were plated on kanamycin-containing agar plates to analyze the *Ds* segregation ratio. The progeny from self-pollinated 34 out of 40 transformant lines segregated in an increased ratio of Kan^R: Kan^S, compared to those from self-crossed *attmem18*/+ controls (Table S3). The aniline blue staining assays showed that the transgenic *attmem18* pollen grains exhibited a normal callose distribution pattern like wild type pollen grains (Figure S1). Furthermore, the *in vitro* pollen germination rates of the transformed *attmem18* lines were increased

(Figure 3B–D) to the values similar to that of wild type pollen. These results demonstrated that the defects in pollen tube growth could be complemented by the introduction of the wild type *AtTMEM18* genomic DNA fragment.

AtTMEM18 is expressed in the tissues active in cell growth and differentiation

The expression pattern of *AtTMEM18* was first analyzed by RT-PCR and Northern blotting hybridization using the RNAs extracted from different wild type plant tissues including seedlings, roots, stems, leaves, flowers, and siliques. The expression of *AtTMEM18* were detected mainly in roots and inflorescences, weaker in seedlings, leaves and siliques (Figure 4A, B), suggesting that *AtTMEM18* was a constitutive expression gene.

The expression pattern of *AtTMEM18* was further examined by promoter activity assay. The *AtTMEM18* promoter was fused to *GUS* reporter gene and introduced into wild type plants. The GUS activity was detected mainly in root tips, the cotyledon of seedlings, mature anthers and pollen tubes (Figure 4C–I), consistent with the results from RT-PCR and Northern blotting hybridization. These results indicated that *AtTMEM18* is constitutively expressed in many tissues, with higher levels in the tissues active in cell growth and differentiation.

The *attmem18* also affected the development of other vegetative tissues

As mentioned above, *attmem18* disrupts the male gameto-phytic function. No *attmem18* homozygous plant was
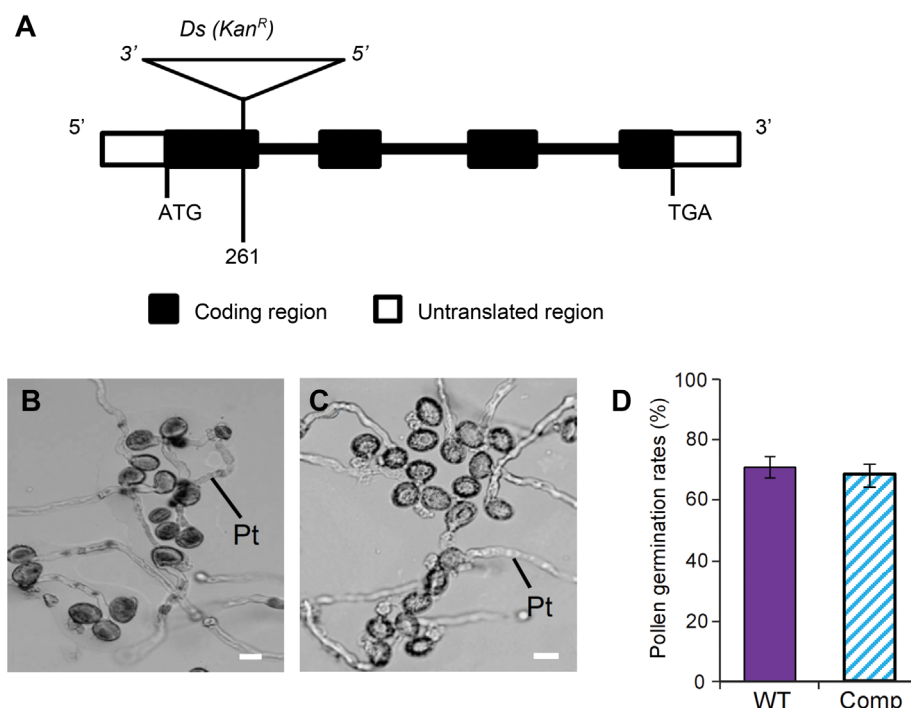
Figure 3. Molecular characterization of *attmem18* mutant
(**A**) The organization of the *AtTMEM18* gene, showing the *Ds* element insertion site. (**B, C**) The *in vitro* germination of pollen grains from wild type (**B**) and complemented plants (**C**). (**D**) Pollen germination rates of the wild type (WT) and the complemented (Comp) plants. Bars = 20 μm.

A

B
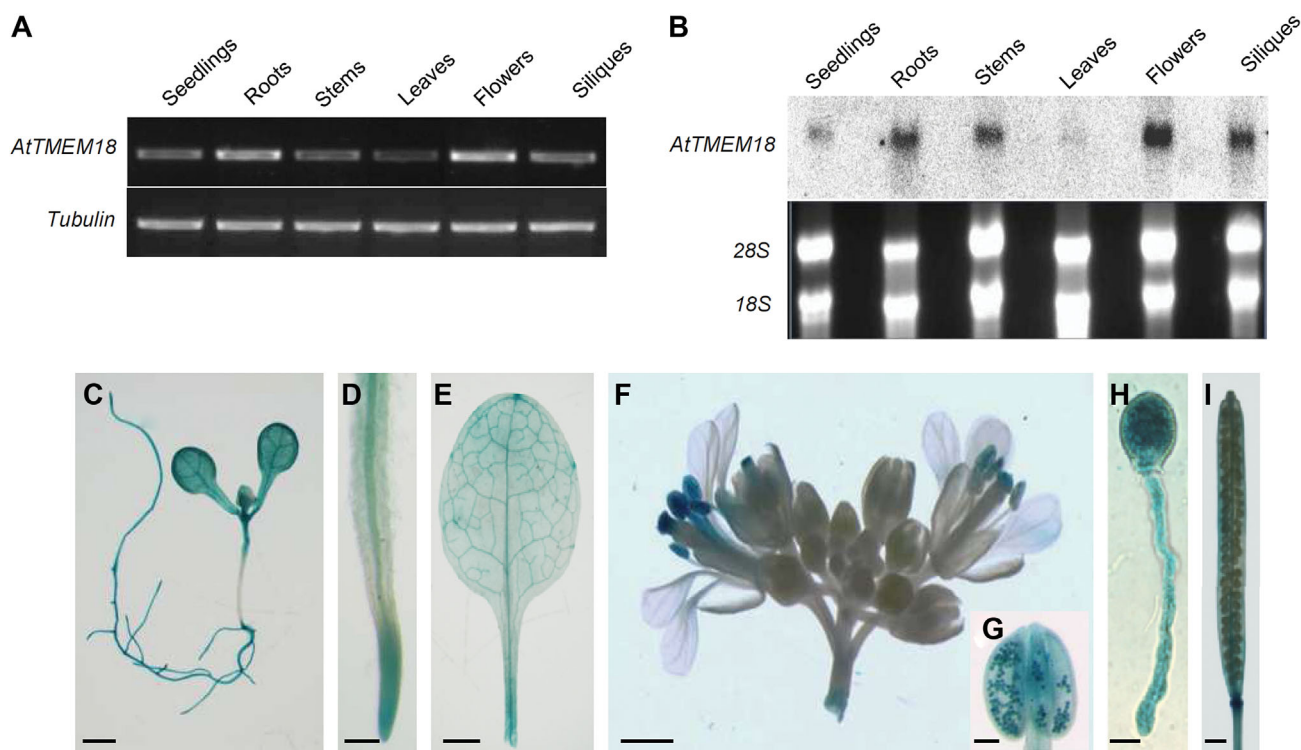
**Figure 4. Expression patterns of *AtTMEM18***

(**A, B**) RT-PCR assay and Northern-blotting, comparing the *AtTMEM18* mRNA levels in seedlings, roots, stems, leaves, flowers and siliques. (**C–I**) GUS activity in seedling (**C**), root (D), leaf (**E**), inflorescence (**F**), anther (**G**), pollen tube (**H**) and silique (**I**) from transgenic wild type plants carrying the p*AtTMEM18:GUS* construct. Bars = 1 mm in (**C**) and (**E**), 0.5 mm in (**F**) and (**I**), 0.1 mm in (**D**) and (**G**), 10 μm in (**H**).

obtained for further investigation of *AtTMEM18* function. To further examine the impact of *attmem18* on vegetative development, we performed the pollen rescue experiments using promoter of the pollen-specific gene *LAT52* (Muschietti et al. 1994) fused with *AtTMEM18* coding region. The resulting p*LAT52:AtTMEM18* construct was introduced into *attmem18*/+ mutant plants. The seeds from self-pollinated T1 transgenic plants were planted on agar plates containing kanamycin. The progeny from the self-pollinated pollen-rescued plants (*attmem18*/+; p*LAT52:AtTMEM18*/+) segregated in a rate of approximately 2 Kan^R : 1 Kan^S, indicating that the construct (p*LAT52:AtTMEM18*) could restore *attmem18* gametophytic function (Table S3). The pollen-rescued lines, which were heterozygous for the *Ds* insertion and homozygous for the T-DNA insertion (*attmem18*/+ p*LAT52:AtTMEM18*/p*LAT52:AtT-MEM18*) were generated and selected for further assays. In the progeny from self-pollinated pollen-rescued plants, approximately 25% (247/1,014) of the seedlings were stunted, compared to wild type seedlings. The hypocotyls, roots and cotyledons of the pollen-rescued seedlings were shorter (Figure 5B–D), compared to those of wild type. When these stunted seedlings developed into mature plants, the height of plants and length of siliques were shorter than those of wild type plants (Figure 5E). The clarified root tips and root paraffin cross sections of the pollen-rescued *attmem18* seedlings

showed that the structures of the root cells were drastically disordered (Figure 5G, K) compared to those of wild type plants (Figure 5F, J). SEM and paraffin cross section observation showed that the epidermal cells of the hypocotyl in pollen-rescued *attmem18* seedlings were distorted (Figure 5I, M). The siliques of pollen-rescued *attmem18* plants were shorter, in which seed set often occurred only in the upper halves of the siliques (Figure 5N, O). When the pollen grains from pollen-rescued *attmem18* plants were pollinated to wild type pistils, the resulting pollen tubes could grow to the bottom of the pollinated wild type pistils (Figure 5P). In contrast, when the wild type pollen grains were pollinated to the pistils of the pollen-rescued *attmem18* plants, the wild type pollen tubes could grow into style, but could not elongate to the bottom of the pistil (Figure 5Q). These results suggested that the p*LAT52:AtTMEM18* construct only specifically restored the gametophytic function, but did not restore silique development. Therefore, the pollen-rescued mutant materials could be used to further study the impact of *attmem18* on vegetative development.

To examine the impact of the *attmem18* on silique development, the paraffin section of transmitting tissue of pollen-rescued *attmem18* plants were observed. The results showed that the style diaphragm of pollen-rescued *attmem18* siliques was not fused, compared to the wild type siliques
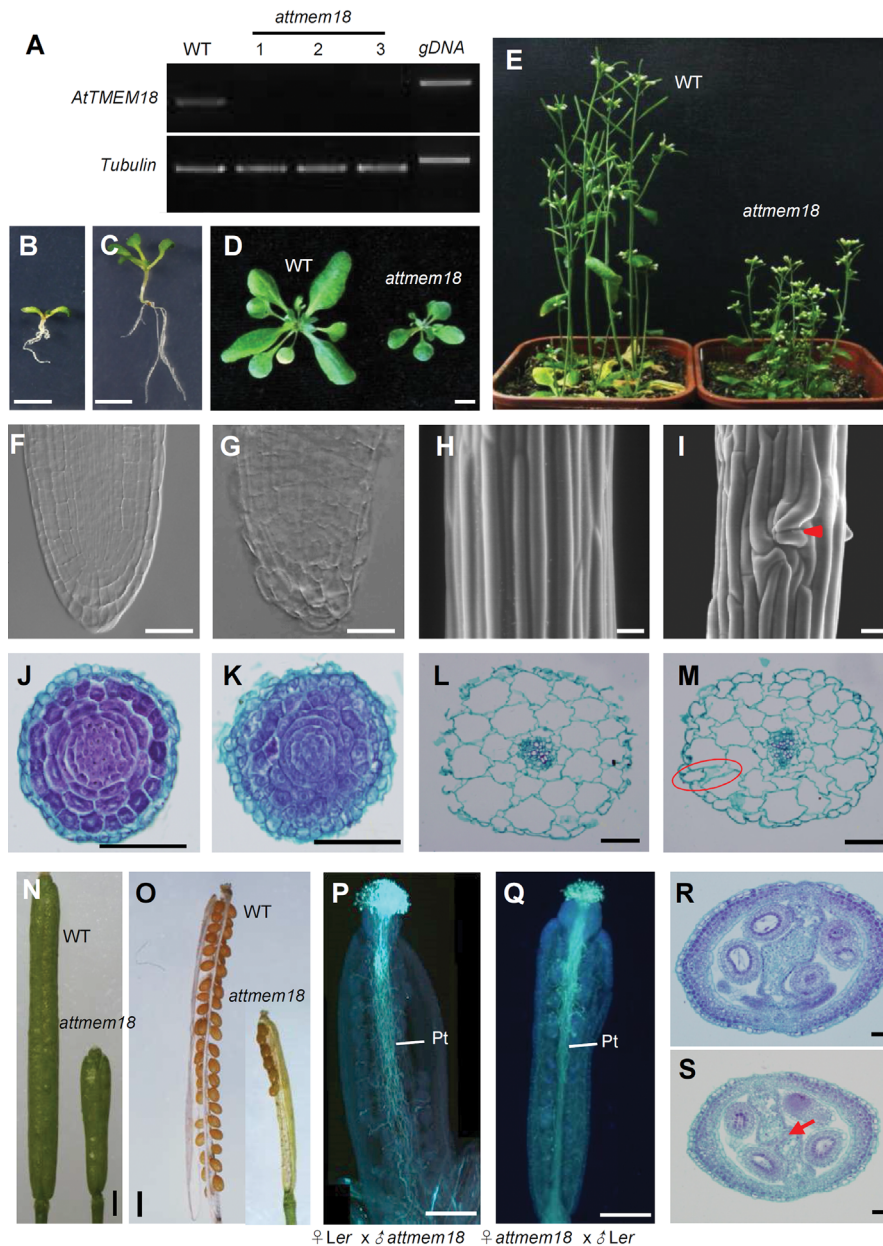
Figure 5. Phenotypic characterization of the pollen-rescued *attmem18* mutants

(**A**) Expression levels of *AtTMEM18* were drastically reduced in the pollen-rescued *attmem18* homozygous seedlings as revealed by RT-PCR. (**B, C**) A 10-d-old pollen-rescued *attmem18* homozygous seedling (**B**), compared with the 10-d-old wild type seedling (**C**) under the same growth conditions. (**D**) A mature pollen-rescued *attmem18* homozygous plant compared with wild type plant (WT) under the same growth conditions. (**E**) The flowering pollen-rescued *attmem18* homozygous plants compared with wild type plants (WT) under the same growth conditions. (**F**) A clarified wild type root tip, showing the typical cell organization pattern. (**G**) A clarified pollen-rescued *attmem18* homozygous root tip, showing the defect in the cell morphology and organization. (**H, I**) The SEM images of hypocotyl epidermal cells in wild type seedlings (**H**) and pollen-rescued *attmem18* homozygous seedling (**I**). The red arrow indicates the distorted epidermal cell organization. (**J, K**) The cross sectioning images of wild type root (**J**) and pollen-rescued *attmem18* homozygous root (**K**). (**L, M**) Comparison of the paraffin cross-sections between wild type hypocotyl (**L**) and pollen-rescued *attmem18* homozygous hypocotyl (**M**). The red oval indicates irregularly hypocotyl cells. (**N**) Comparison of the siliques at the 7th day after pollination (DAP) between wild type and pollen-rescued *attmem18* homozygous plants. The silique of homozygous *attmem18* mutant was much shorter than that of wild type. (**O**) Mature siliques from wild type plants and *attmem18* plants. (**P**) The growth of *attmem18* pollen tubes in the wild type (L*er*) at 12 DAP. (**Q**) The growth of wild type pollen tubes in the *attmem18* silique at 12 DAP. (**R, S**) Comparison of paraffin cross section in wild type pistil (**R**) and *attmem18* pistil (**S**). The red arrow indicates the unfused style diaphragm in *attmem18* pistil. Bars = 500 μm in (**B**) to (**D**), (**N**) and (**O**), 50 μm in (**F**) to (**M**), (**P**) to (**S**).

(Figure 5R, S). These results indicated that the cell morphogenesis in pollen-rescued *attmem18* mutant siliques were affected. PCR assays using DNA from the defective pollen-rescued *attmem18* seedlings indicated that they were homozygous for the *attmem18* mutation. RT-PCR assays using the RNAs extracted from the pollen-rescued *attmem18* homozygous seedlings showed that expression of *AtTMEM18* was dramatically reduced in the pollen-rescued *attmem18* seedlings (Figure 5A). Transgenic wild type plants with pLAT52:*AtTMEM18* coding region construct were examined as a negative control, no defective plants were found in these transgenic plants in wild type background. Therefore, the *attmem18* mutation also affected vegetative development in *Arabidopsis*.

AtTMEM18 protein is located around nucleus

AtTMEM18 protein has 163 amino acid residues in length and contains three predicted transmembrane domains (http://www.cbs.dtu.dk/services). It shares similarities with the proteins from many species in eucaryon except yeast and nematode, but not in bacteria. In particular, AtTMEM18 shares 72% similarity with LOC100527513 (*Glycine max*) and POPTRDRAFT_287702 (*Populus trichoca*), 59% similarity with LOC100283849 (*Zea mays*), 53% similarity with Os05g0432500 (*Oryza sativa*) and 34% similarity with Transmembrane 18 (*Mus musculus*) and TMEM18 (*Homo sapiens*) (Figure 6A). The phylogenetic tree analysis showed that TMEM18 proteins could be clustered into animal and plant groups, respectively (Figure 6B). AtTMEM18 belongs to the plant group.

To investigate the subcellular localization of AtTMEM18, 1.0-kb promoter of *AtTMEM18* was fused to the *AtTMEM18* genomic coding region and the coding sequence of green fluorescent protein (GFP). The resulting construct pAtTMEM18:gAtTMEM18-GFP was introduced into wild type and heterozygous *attmem18*/+ plants, respectively. Genetic analysis showed that the progeny from self-pollination of the resulting transgenic heterozygous (*attmem18*/+) segregated in a Kan[R]: Kan[S] ratio of up to 2:1 (Table S3), indicating that the AtTMEM18-GFP fusion protein could function normally. The GFP signals were observed in roots, pollen grains at the unicellular to tricellular stages and pollen tubes. In unicellular pollen grains, the GFP signals were detected around the unique nuclei (Figure 7A). In the bicellular pollen grains, the GFP signals appeared around the vegetative and generative nuclei (Figure 7B). In the tricellular pollen grains, the GFP signals were located around the vegetative and two sperm nuclei (Figure 7C). In the germinating pollen grains, the GFP signals were detected around the vegetative and sperm nuclei in the growing pollen tubes (Figure 7D). In the root hair, the GFP signals were expressed around the nuclei (Figure 7E).

To examine whether the protein localization was related to the introns of the gene, another construct was generated by replacing the genomic coding sequence (gAtTMEM18) with the *AtTMEM18* cDNA. The resulting pAtTMEM18:cAtTMEM18-GFP construct was also introduced into heterozygous *attmem18* (*attmem18*/+) plants. The progeny from the self-pollinated transgenic *attmem18*/+ plants segregated in a ratio of 1 Kan[R]:1 Kan[S], like the progeny from the self-pollinated nontransgenic *attmem18*/+ plants, indicating that pAtTMEM18:cAtTMEM18-GFP could not restore the fertility of *attmem18* mutant. The GFP signal was detected in the pAtTMEM18:cAtTMEM18-GFP transgenic pollen grains and

roots (Figure 7F–I) roots and pollen grains. In the transgenic root hairs, the GFP signals could be detected around the nucleus like those in the pAtTMEM18:gAtTMEM18-GFP transgenic plants (Figure7I). During the periods of pollen development, however, the GFP signals were appeared only around the vegetative cell nuclei (Figure 7F–H), differently from those in the pAtTMEM18:gAtTMEM18-GFP transgenic pollen grains in which GFP signals were located not only around the vegetative nuclei but also around the generative nuclei at the bicellular stage or around the sperm nuclei at the mature pollen stage. These results indicated that the introns of the *AtTMEM18* was related to its expression in generative and sperm nuclei in *Arabidopsis*.

To further examine which intron was involved in its expression regulation in *AtTMEM18*, deletion assays were performed. *AtTMEM18* gene has three introns (Figure S2A). As shown in Figure S2A, six constructs were generated for the assays. The resulting six constructs were introduced into *attmem18*/+ plants, respectively. The genetic analyses showed that the progeny from all the six construct transgenic *attmem18*/+ plants segregated in a ratio of approximately 2 Kan[R]: 1 Kan[S] (Table S3), indicating that all six constructs could complement the fertility of *attmem18* mutant. The GFP signals were located around the vegetative and sperm nuclei of the transgenic tricellular pollen grains (Figure S2B). Thus, any one intron of *AtTMEM18* could be enough to enable the correct expression of *AtTMEM18* in the pollen grains.

### Expression of the rice TMEM18 (Os05g0432500) in *attmem18* could complement the *attmem18* mutant phenotype

BlastP search showed that rice (*Oryza sativa*) also has a TMEM18-homologous protein, namely Os05g0432500. To examine whether Os05g0432500 had the same function as AtTMEM18 in *Arabidopsis*, the construct pLAT52:*Os05g0432500* was generated and introduced into *attmem18*/+ mutant plants. The seedlings from the self-pollinated T1 transgenic plants segregated in a ratio of 2 Kan[R]: 1 Kan[S] (Table S3), compared to the 1 Kan[R]: 1 Kan[S] segregation of the seedlings from the self-pollinated non-transgenic *attmem18*/+ mutant plants. The result showed that the rice Os05g0432500 protein could complement the functional loss of AtTMEM18 in *Arabidopsis*.

DISCUSSION

AtTMEM18 is important for pollen tube growth

We report here the functional characterization of *AtTMEM18* that is involved in pollen tube growth. *AtTMEM18* encodes a transmembrane protein, which shares higher similarity with the TMEM18 proteins found in many animal and plant species. In the rat brain, the TMEM18 is located in the nuclear envelope of the neural stem cells (Jurvansuu et al. 2008). The GFP fusion protein assays demonstrated that AtTMEM18 is located around nuclei, implying that it might be also located in the nuclear envelope. However, more direct evidence still is required to address this question.

AtTMEM18 is expressed in the developing pollen grains at the stages from unicellular to mature pollen grains, indicating that it is related to male gametophytic function. The *Ds* insertion in *AtTMEM18* caused defect in pollen germination and pollen

A

B
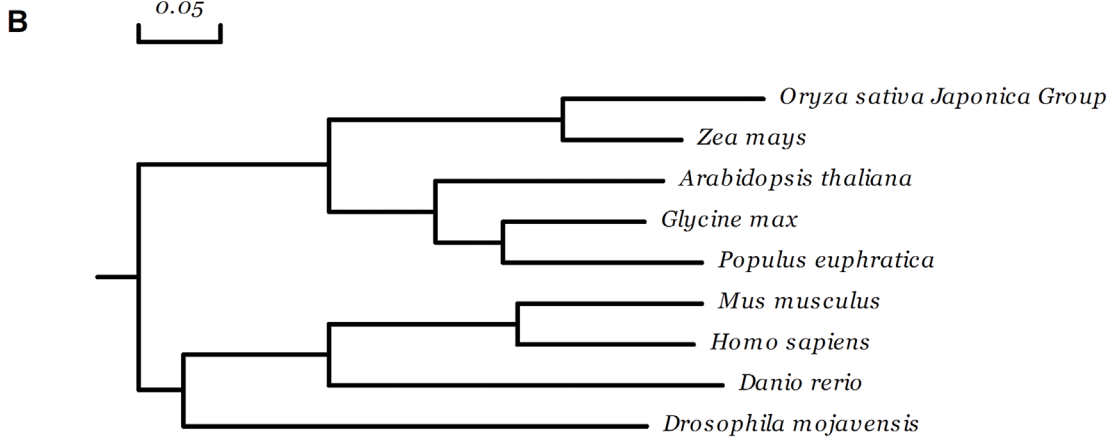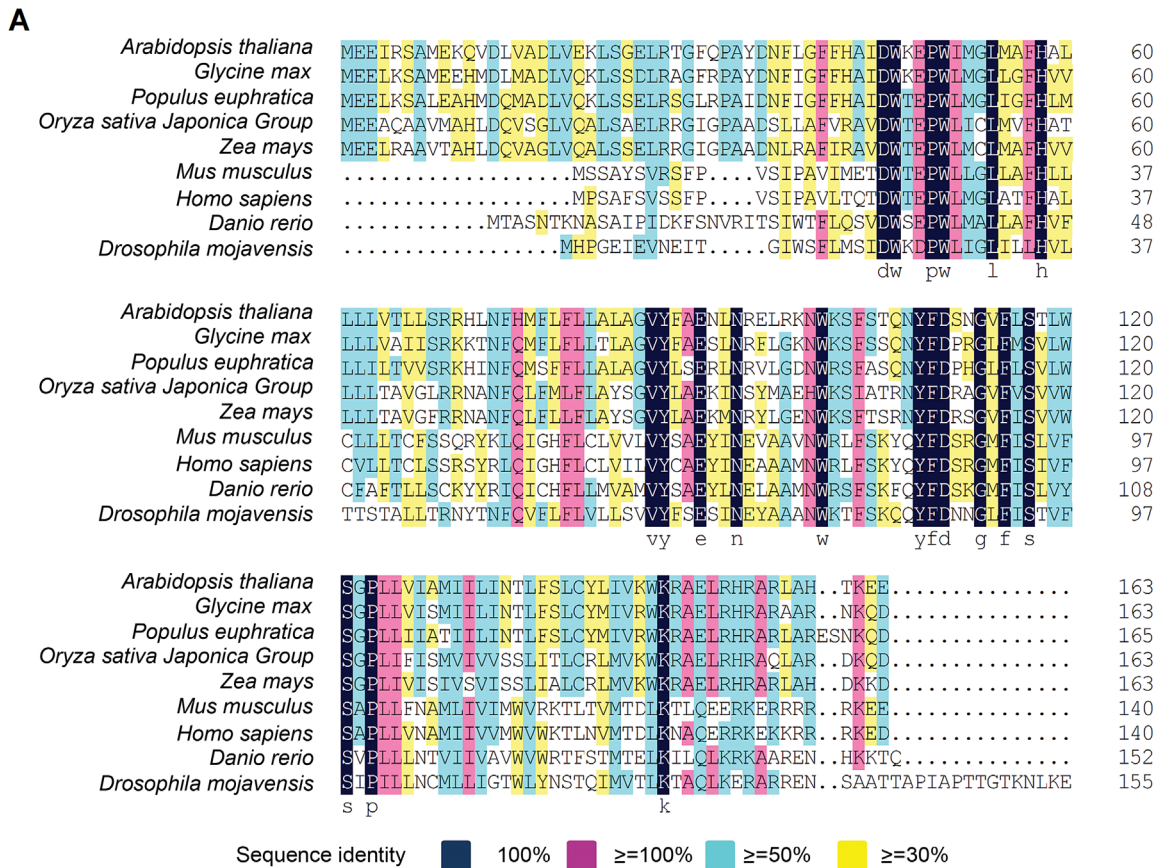
Figure 6. AtTMEM18 shares sequence similarity with many TMEM18 from other species
(**A**) Sequence alignment of AtTMEM18-homologous proteins. (**B**) Phylogenetic analysis of AtTMEM1-homologous proteins. The scale bar represents genetic distance. Species and accession number: *Arabidopsis thaliana*, AT1G34350; *Glycine max*, NP_001237116; *Populus euphratica*, XP_011038158; *Oryza sativa Japonica Group*, Os05g0432500; *Zea mays*, AFW61473; *Mus musculus*, NP_742046; *Homo sapiens*, NP_690047; *Danio rerio*, NP_001005601; *Drosophila mojavensis*, EDW08271.

tube growth, but did not affect the division of generative cells and morphology of mature pollen grains. Thus, AtTMEM18 protein is important for pollen germination and pollen tube growth, but may not be essential for pollen formation.

The *attmem18* pollen tubes became swollen. It has been reported that defects in pollen tube wall components can cause the pollen tube wall to be unstable, resulting in swollen pollen tubes (Wang et al. 2013). Our histological assays showed that the *attmem18* pollen grains exhibited a dotted callose distribution pattern before germination, different from those in wild type pollen grains. In wild type, callose appears prolifically at two stages, namely
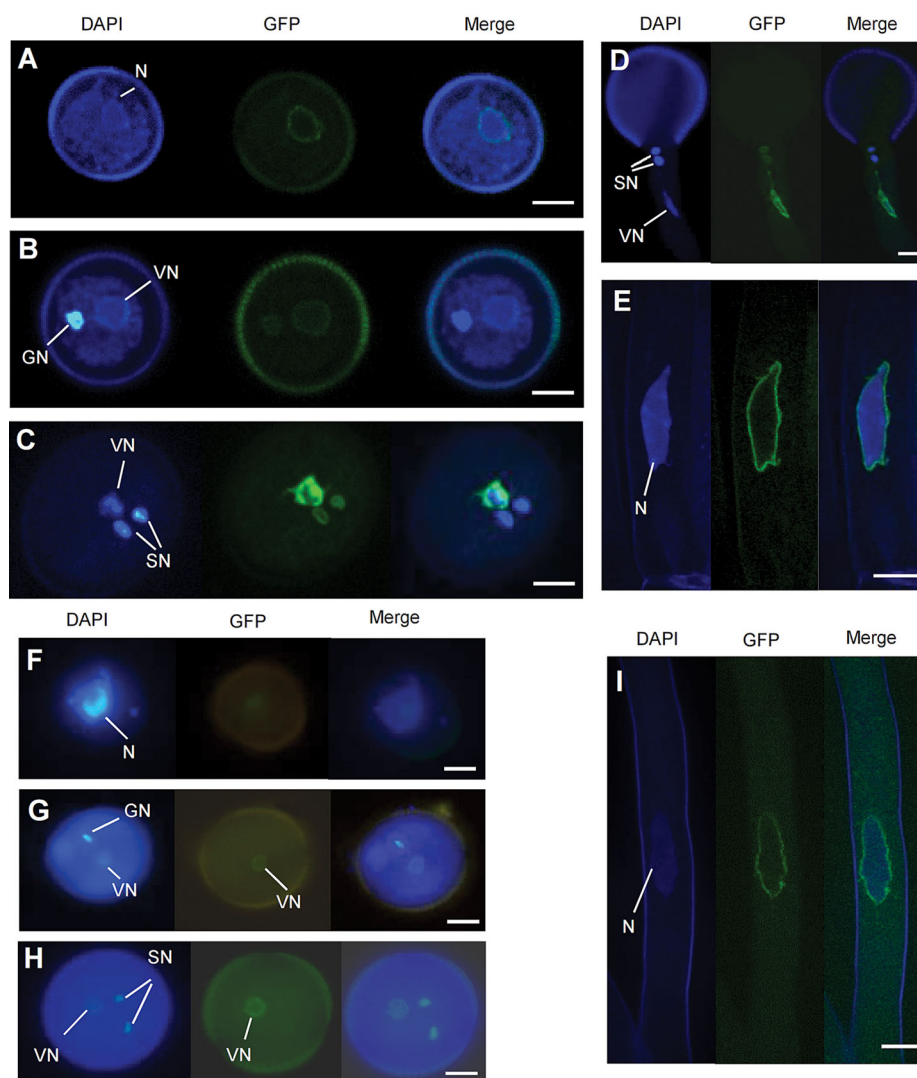
Figure 7. Subcellular localization of AtTMEM18-GFP

(**A–E**) The GFP signals were located around the nuclei in unicellular pollen grain (**A**), bicellulare pollen grain (**B**), tricellulare pollen grain (**C**), pollen tube (**D**) and root hair (**E**) from the p*AtTMEM18*:g*AtTMEM18-GFP* transgenic plants. (**F–I**) The GFP signals were located around the nuclei in the unicellular pollen grain (**F**), bicellulare pollen grain (**G**), tricellulare pollen grain (**H**) and root hair (**I**) from p*AtTMEM18*:c*AtTMEM18-GFP* transgenic plants. GN, generative nuclei; N, nuclei; VN, vegetative nuclei; Bars = 5 μm.

tetrad stage and pollen tube growth stage after germination. At the tetrad stage, the callose walls were formed to separate and protect the microspores. During emergence of the pollen tubes, the callose deposition could be detected at the rim of the germination aperture (Li et al. 1999b). Then, in pollen tube, callose can be steadily detected in the distal region, which is confined to the inner wall layer and to transverse walls named a plug (Ferguson et al. 1998; Li et al. 1999b). The callose plug is consistent with its role in resisting tension stresses (Chebli et al. 2012). According to these results, the mature pollen grains did not synthesize callose before germination. The irregular callose deposition in the inner wall of *attmem18* pollen gains suggested *AtTMEM18* may play roles in the time-control of callose synthesis. Therefore, we speculate that the premature callose synthesis

in ungerminated pollen grain may be the major cause for the abnormal germination. Furthermore, our results also showed that the callose distribution in the swollen *attmem18* pollen tubes were significantly different from those of wild type pollen tube. When *attmem18* pollen grains were cultured *in vitro*, no callose plugs were formed in the swollen mutant pollen tubes after germination although the dotted callose deposition still appeared in the inner wall of the pollen grains. Moreover, the pollen tube walls lacked or had less callose deposition. Therefore, we speculated that *AtTMEM18* may be involved in pollen tube growth through controlling deposition or synthesis of callose in pollen grains and pollen tubes. There could be two possibilities for the mechanism that AtTMEM18 controls deposition or synthesis of the callose. One is that AtTMEM18 may be involved in the

regulation of expression of the genes related to callose biosynthesis. The data supporting this hypothesis is that the C-terminal of the TMEM18 proteins in animal could form homo-polymer, bind to DNA of the chromosome and repress transcription of certain genes in the nucleus (Jurvansuu and Goldman 2011). Another possibility is that AtTMEM18 may participate in the transportation of the proteins related to callose biosynthesis or deposition. Nevertheless, more studies are still required to address how AtTMEM18 controls the deposition of callose to the walls of pollen grains and pollen tubes.

AtTMEM18 may influence the morphogenesis of the vegetative cells in *Arabidopsis*

The pollen-rescue assays showed that the *attmem18* also severely affected the development of the vegetative tissues, including hypocotyls, cotyledon, roots, leaves, siliques, resulting in shorter plants and reduction in seed set. The sectioning of the tissues showed that the diaphragm was not fused in the mutant siliques. The shapes of the cells in the distorted tissues including siliques and roots were altered. These results indicate that TMEM18 is important for normal plant cell growth, especially for cell morphogenesis.

The introns of *AtTMEM18* is essential for its expression in generative cells of pollen grains

In the GFP fusion protein assays for AtTMEM18 protein localization, the p*AtTMEM18*:c*AtTMEM18-GFP* could not complement the male sterile phenotype of *attmem18* mutant, but the p*AtTMEM18*:g*AtTMEM18-GFP* could. In p*AtTMEM18*:c*AtTMEM18-GFP*, the *AtTMEM18* cDNA was used, which lacked the three introns of *AtTMEM18*, whereas in p*AtTMEM18*:g*AtTMEM18-GFP*, the genomic coding sequences was fused to GFP, which contained three introns. Therefore, the results indicated that the introns are essential for the expression of *AtTMEM18* function on male fertility. In the p*AtTMEM18*:g*AtTMEM18-GFP* transgenic *attmem18*/+ plants, the AtTMEM18-GFP was expressed around the nuclei of both vegetative cells and two sperm cells, while in p*AtTMEM18*:c*AtTMEM18-GFP* transgenic *attmem18*/+ plants, the AtTMEM18-GFP was expressed only around the nucleus of the vegetative cell, but not in those of the sperm cells. Therefore, the introns of *AtTMEM18* are essential for its expression in sperm cells. Further deletion assays for the introns demonstrated that either of the three introns is enough to ensure the expression of *AtTMEM18* in sperm cells, which could restore the male gametophytic function of *attmem18* mutant. Taken together, expression of *AtTMEM18* in sperm cells is essential for its function on male gametophytic function, and the introns of *AtTMEM18* are required to ensure its expression in sperm cells.

It is still worthy to point out that when the pollen specific promoter *LAT52* was used to drive the expression of *AtTMEM18* in pollen grain and pollen tubes, the progeny from the self-pollinated p*LAT52*:c*AtTMEM18-GFP* transgenic *attmem18*/+ mutant plants segregated in ratio of approximately 2 Kan^R : 1 Kan^S (data not shown), indicating that p*LAT52*:c*AtTMEM18-GFP* also could restore the male gametophytic function of *attmem18*. The green fluorescence of AtTMEM18-GFP was distributed in the whole pollen grains, included the vegetative cell and sperm cells (Figure S3). This result demonstrated that

use of *LAT52* promoter also could complement the roles of *AtTMEM18* introns.

The *TMEM18* genes in plants might be different from those in animals

TMEM18 protein is remarkably well conserved across this 1,500 million year evolutionary history (Almén et al. 2010). Surprisingly it has no clear homologs in either yeast or *Caenorhabditis elegans* (Almén et al. 2010). AtTMEM18 shares 72%, 53% and 34% similarity with the homologous proteins of *Populus trichoca*, *Oryza sativa* and *Homo sapien*, respectively. The homologous analysis showed the AtTMEM18 was clustered with the plant group. These results indicated that the functions of TMEM18 proteins might be different between plants and animals. The differences in the structure between TMEM18 and AtTMEM18 were mainly reflected in two aspects. First, the C-terminal of TMEM18 protein has a typical nucleic acid-binding motif (ERRKEKKRRRKED) and has been demonstrated to bind to DNA (Jurvansuu and Goldman 2011). The second significant difference is that there are four cysteine residues in the first and second transmembrane domain of TMEM18. With these four cysteine residues, TMEM18 proteins could form homo-polymer and be located in nuclear envelope, and enable the C-terminal of the protein to bind DNA on the chromosome and repress transcription of certain genes in the nucleus (Jurvansuu and Goldman 2011). In contrast, there were no any typical nucleic acid binding motif in the C-terminal region of AtTMEM18 and other homologous proteins in plants. Furthermore, DNA binding assay showed that AtTMEM18 could not bind to DNA. Moreover, BIFC assay showed that AtTMEM18 also could not form homodimers. In addition, expression of the mouse TMEM18 protein in *attmem18* could not recover the male fertility of the mutant, but expression of the rice homologous gene (*Os05G0432500*) driven by the pollen-specific *LAT52* promoter could restore the male gametophytic fertility of *attmem18*. Taken together, the AtTMEM18 proteins may be functionally different from those in animals.

MATERIALS AND METHODS

Plant materials and mutant isolation

The *Arabidopsis thaliana* plants used in this study were all in Landsberg *erecta* background. The seeds were plated on MS-salt agar plates with or without 50 mg/L kanamycin (Sigma-Aldrich) or 20 mg/L hygromycin (Roche, Basel, Switzerland) at 4 °C for 2 d. Then the seeds were cultured at 22 °C under a light cycle of 16 h light/8 h dark for 10 d. The resulting 10-d-old seedlings were grown into soil in the same growth condition. The generation of *Ds* insertion lines and screen of mutants were performed as described by Sundaresan et al. (1995).

Characterization of *attmem18* mutant phenotype

Morphological observations of pollen grains by SEM were performed as described by Jiang et al. (2005). Pollen viability was examined using Alexander staining (Alexander 1969). DAPI staining of pollen grains was performed as described by Yang et al. (2009).

To examine *in vitro* pollen germination, the pollen grains were plated on the agar-solid pollen germination medium

containing 1 mM KCl, 10 mM CaCl$_2$, 0.8 mM MgSO$_4$, 0.01% H$_3$BO$_3$ and 18% sucrose. Then the pollen plates were incubated at 22–24 °C for 6 h. At least 300 pollen grains were examined to calculate the average germination rates for each sample.

To examine *in vivo* pollen tube growth, the flowers were emasculated one day before anthesis. The being cultured at 22 °C for 6 h, the pollinated pistils were mounted onto the sample platform and quickly examined for the pollen tube growth patterns on the stigma by SEM (HITACHI, S-3400N). On the other hand, the pollinated pistils were collected and fixed in fixing solution (ethanol:acetic acid = 3:1) for 6 h. Then the fixed pistils were softened in 8 M NaOH overnight. After washed with water for several times, the pistils were stained with aniline blue buffer (0.1% aniline blue in 0.1 M K$_2$HPO$_4$-KOH buffer with pH = 11.0) for 2 h in the dark. The pollen tube growth patterns inside the pistils were observed using fluorescence microscopy (LEICA, DM2500, Germany).

Pollen grain immunocytochemistry assay was performed as described by Geitmann et al. (1995).

Localization of *Ds* insertion site in *attmem18* mutant

The flanking sequence adjacent to the *Ds* element was obtained by TAIL-PCR (Liu et al. 1995; Liu and Whittier 1995). Extraction of the *attmem18* genomic DNA and TAIL-PCR were performed using *Ds*/AD primer sets, as described previously (Yang et al. 1999). The *Ds* insertion was confirmed by conventional PCR using *Ds*-specific primers Ds5-3 (Table S4) paired with the gene-specific primer AtTMEM18-Ds-3′ (Table S4). The *Ds* insertion site was determined by sequencing of the resulting flanking DNA fragments.

Complementation experiments

The 5′ upstream sequence and genomic DNA of *AtTMEM18* was amplified using *rTaq* (TaKaRa, Japan) with primers AtTMEM18-g-5′ and AtTMEM18-g-3′ (Table S4) and verified by sequencing. The resulting DNA fragment was cloned into the Ti-derived binary vector pCAMBIA1300 (CAMBIA, Australia) and introduced into the *attmem18* heterozygous mutant plants by *Agrobacterium tumefaciens* (strain GV3101)-mediated infiltration method (Bechtold and Pelletier 1998). The transformant plants were selected on MS medium supplemented with 50 mg/L kanamycin and 20 mg/L hygromycin. The selected transgenic plants were transferred into soil to produce T2 seeds. The T2 seeds were germinated on kanamycin-containing MS agar plates to evaluate the complementation efficiency by analyzing the segregation ratio of kanamycin resistance.

The pollen rescue experiment was performed by pollen-specific expression of *AtTMEM18* coding region in *attmem18*/+ plants. The coding region of *AtTMEM18* was amplified using *rTaq* with primers AtTMEM18-c-5′ and AtTMEM18-c-3′ (Table S4). The *LAT52* promoter fragment was obtained from the plasmid pUCLNGFP2 (a gift from Dr. Zhenbiao Yang, Department of Botany and Plant Science, University of California at Riverside, CA). The resulting DNA fragment was cloned into Ti-derived binary vector pCAMBIA1300. The resulting constructs were transformed into *attmem18*/+ plants. The selection and segregation analysis of transformant plants was performed as described above.

The total RNA of rice (*Oryza sativa*) seedlings was extracted with cetyltrimethylammonium bromide (CTAB)

solution (Yu and Goh 2000). Reverse transcription was performed using alfalfa mosaic virus reverse transcriptase (AMV, TaKaRa, http://www.takara-bio.com/). The coding region of *Os05g0432500* was amplified using *rTaq* with primers Os-c-5′ and Os-c-3′ (Table S4). The pLAT52:*Os05g0432500* construct was transformed into *attmem18*/+ plants. The selection and genetic analysis of transformant plants was performed as described above.

Assays for *AtTMEM18* expression pattern

The seedlings, roots, stems, leaves, flowers and siliques were harvested from 2-week-old seedlings and 4-week-old flowering plants, respectively. The total RNAs were extracted with cetyltrimethylammonium bromide (CTAB) solution (Yu and Goh 2000). Reverse transcription was performed using alfalfa mosaic virus reverse transcriptase (AMV, TaKaRa, http://www.takara-bio.com/). TUBULIN cDNA was used as an internal control to normalize the amount of cDNA templates. The primers TUBULIN-RT-5′ and TUBULIN-RT-3′ (Table S4) were used to amplify the TUBULIN cDNA fragment. The primers AtTMEM18–RT-5′ and AtTMEM18–RT-3′ (Table S4) were used to assess the expression level of AtTMEM18 as previously described by Yang et al. (2009).

In Northern blotting hybridization, *AtTMEM18* gene-specific probe was amplified by *rTaq* using the primers AtTMEM18–RT-5′ and AtTMEM18–RT-3′ (Table S4). The RNA probes were labeled using the DIG RNA labeling kit (Roche, Indianapolis, IN, USA) as described by the supplier. RNA gel blotting hybridizations were performed following the instructions of the DIG system and DIG application manual provided by the supplier.

The *AtTMEM18* promoter was amplified using *rTaq* with primers AtTMEM18-p-5′ and AtTMEM18-p-3′ (Table S4). After verified by sequencing, the fragment was subcloned upstream of the *GUS* reporter gene in Ti-derived binary vector pCAMBIA1300 to generate the expression cassette p*AtTMEM18*:*GUS*. The resulting construct was introduced into the wild type plants by *Agrobacterium tumefaciens* (strain GV3101)-mediated infiltration method (Bechtold and Pelletier 1998). The transformant plants were selected on MS medium supplemented with 20 mg/L hygromycin. The selected transgenic plants were transferred into soil to produce T2 seeds. GUS staining of T2 plants tissues were performed as described previously (Sundaresan et al. 1995; Yang et al. 1999).

Phenotypic characterization of pollen-rescued plants

For paraffin sectioning, the roots, stems, leaves and siliques of the pollen-rescued *attmem18* plants and wild type plants were fixed in 50% formalin-acetic acid-alcohol (FAA) solution and processed according to Shi et al. (2005) and Yang et al. (1999). The observation of the clarified root tips were as described by Yang et al. (1999).

Assays for protein subcellular localization

The *AtTMEM18* promoter fragment was amplified using *rTaq* (TaKaRa) with primers AtTMEM18-P-5′ and AtTMEM18-P-3′ (Table S4). The *AtTMEM18* genomic DNA fragment without the stop codon was amplified by *rTaq* using primers AtTMEM18-g-5′-2 and AtTMEM18-g-3′-2 (Table S4). The *AtTMEM18* coding region fragment without the stop codon

was amplified using r*Taq* with primers AtTMEM18-c-5′ and AtTMEM18-c-3′ (Table S4). After verified by sequencing, the *AtTMEM18* promoter and genomic DNA fragments were subcloned in front of the *NOS* terminator sequence (T$_{NOS}$) in the modified pCAMBIA1300 vector which contained GFP coding region, resulting in a p*AtTMEM18:gAtTMEM18-GFP*:T$_{NOS}$ construct. The p*AtTMEM18:cAtTMEM18-GFP*:T$_{NOS}$ construct was generated in the same way. The p*AtTMEM18:gAtTMEM18-GFP*:T$_{NOS}$ and p*AtTMEM18:cAtTMEM 18-GFP*:T$_{NOS}$ constructs were introduced into *attmem18*/+ and wild type plants, respectively. The transformant plants were selected using 50 mg/L kanamycin and 20 mg/L hygromycin. The subcellular localization of AtTMEM18-GFP fusion protein in the roots, pollen grains and pollen tubes was visualized under a confocal microscope (LSM510, Carl Zeiss, Germany, http://www.zeiss.com).

ACKNOWLEDGEMENTS

AUTHOR CONTRIBUTIONS

Conceived and designed the experiments: D.Y., X.Y.D. and K.Z.Y. Performed the experiments: X.Y.D., K.Z.Y., Z.X.M., L.Q.C. and X.Q.Z. Analyzed the data: X.Y.D., K.Z.Y. and D.Y. Wrote the paper: D.Y., X.Y.D., K.Z.Y., and J.R.B.

REFERENCES

Alexander M (1969) Differential staining of aborted and nonaborted pollen. **Stain Technol** 44: 117–122

Almén MS, Jacobsson JA, Shaik JH, Olszewski PK, Cedernaes J, Alsiö J, Sreedharan S, Levine AS, Fredriksson R, Marcus C (2010) The obesity gene, TMEM18, is of ancient origin, found in majority of neuronal cells in all major brain regions and associated with obesity in severely obese children. **BMC Med Genet** 11: 58

Bechtold N, Pelletier G (1998) In planta *Agrobacterium*-mediated transformation of adult *Arabidopsis thaliana* plants by vacuum infiltration. **Methods Mol Biol** 82: 259–266

Bedinger P (1992) The remarkable biology of pollen. **Plant Cell** 4: 879

Chebli Y, Kaneda M, Zerzour R, Geitmann A (2012) The cell wall of the *Arabidopsis* pollen tube — spatial distribution, recycling, and network formation of polysaccharides. **Plant Physiol** 160: 1940–1955

Dardelle F, Lehner A, Ramdani Y, Bardor M, Lerouge P, Driouich A, Mollet J-C (2010) Biochemical and immunocytological characterizations of *Arabidopsis* pollen tube cell wall. **Plant Physiol** 153: 1563–1576

Dong X, Hong Z, Sivaramakrishnan M, Mahfouz M, Verma DPS (2005) Callose synthase (CalS5) is required for exine formation during

microgametogenesis and for pollen viability in *Arabidopsis*. **Plant J** 42: 315–328

Edlund AF, Swanson R, Preuss D (2004) Pollen and stigma structure and function: The role of diversity in pollination. **Plant Cell** 16: S84–S97

Ferguson C, Teeri T, Siika-Aho M, Read S, Bacic A (1998) Location of cellulose and callose in pollen tubes and grains of *Nicotiana tabacum*. **Planta** 206: 452–460

Geitmann A, Hudák J, Vennigerholz F, Walles B (1995) Immunogold localization of pectin and callose in pollen grains and pollen tubes of *Brugmansia suaveolens* — implications for the self-incompatibility reaction. **J Plant Physiol** 147: 225–235

Geitmann A, Steer M (2006) The architecture and properties of the pollen tube cell wall. *The Pollen Tube*. Springer. pp. 177–200

Guan Y, Guo J, Li H, Yang Z (2013) Signaling in pollen tube growth: Crosstalk, feedback, and missing links. **Mol Plant** 6: 1053–1064

Hülskamp M, Kopczak SD, Horejsi TF, Kihl BK, Pruitt RE (1995) Identification of genes required for pollen – stigma recognition in *Arabidopsis thaliana*. **Plant J** 8: 703–714

Harholt J, Suttangkakul A, Scheller HV (2010) Biosynthesis of pectin. **Plant Physiol** 153: 384–395

Hepler PK, Rounds CM, Winship LJ (2013) Control of cell wall extensibility during pollen tube growth. **Mol Plant** 6: 998–1017

Iwano M, Entani T, Shiba H, Kakita M, Nagai T, Mizuno H, Miyawaki A, Shoji T, Kubo K, Isogai A (2009) Fine-tuning of the cytoplasmic Ca^{2+} concentration is essential for pollen tube growth. **Plant Physiol** 150: 1322–1334

Jiang L, Yang SL, Xie LF, San Puah C, Zhang XQ, Yang WC, Sundaresan V, Ye D (2005) *VANGUARD1* encodes a pectin methylesterase that enhances pollen tube growth in the *Arabidopsis* style and transmitting tract. **Plant Cell** 17: 584–596

Johnson MA, Preuss D (2002) Plotting a course: Multiple signals guide pollen tubes to their targets. **Dev Cell** 2: 273–281

Jurvansuu J, Zhao Y, Leung DS, Boulaire J, Yu YH, Ahmed S, Wang S (2008) Transmembrane protein 18 enhances the tropism of neural stem cells for glioma cells. **Cancer Res** 68: 4614–4622

Jurvansuu JM, Goldman A (2011) Obesity risk gene *TMEM18* encodes a sequence-specific DNA-binding protein. **PLoS ONE** 6: e25317

Kim S, Mollet J-C., Dong J, Zhang K, Park S-Y, Lord EM (2003) Chemocyanin, a small basic protein from the lily stigma, induces pollen tube chemotropism. **Proc Natl Acad Sci** 100: 16125–16130

Krichevsky A, Kozlovsky SV, Tian GW, Chen MH, Zaltsman A, Citovsky V (2007) How pollen tubes grow. **Dev Biol** 303: 405–420

Lancelle SA, Hepler P (1992) Ultrastructure of freeze-substituted pollen tubes of *Lilium longiflorum*. **Protoplasma** 167: 215–230

Lennon K, Lord E (2000) In vivo pollen tube cell of *Arabidopsis thaliana* I. Tube cell cytoplasm and wall. **Protoplasma** 214: 45–56

Li H, Bacic A, Read SM (1999a) Role of a callose synthase zymogen in regulating wall deposition in pollen tubes of *Nicotiana alata* Link et Otto. **Planta** 208: 528–538

Li H, Lin Y, Heath RM, Zhu MX, Yang Z (1999b) Control of pollen tube tip growth by a Rop GTPase-dependent pathway that leads to tip-localized calcium influx. **Plant Cell** 11: 1731–1742

Liu YG, Mitsukawa N, Oosumi T, Whittier RF (1995) Efficient isolation and mapping of *Arabidopsis thaliana* T-DNA insert junctions by thermal asymmetric interlaced PCR. **Plant J** 8: 457–463

Liu YG, Whittier RF (1995) Thermal asymmetric interlaced PCR: Automatable amplification and sequencing of insert end fragments

from P1 and YAC clones for chromosome walking. **Genomics** 25: 674–681

Lord EM, Russell SD (2002) The mechanisms of pollination and fertilization in plants. **Annu Rev Cell Dev Biol** 18: 81–105

Michard E, Alves F, Feijó JA (2009) The role of ion fluxes in polarized cell growth and morphogenesis: The pollen tube as an experimental paradigm. **Int J Dev Biol** 53: 1609

Muschietti J, Dircks L, Vancanneyt G, McCormick S (1994) LAT52 protein is essential for tomato pollen development: Pollen expressing antisense LAT52 RNA hydrates and germinates abnormally and cannot achieve fertilization. **Plant J** 6: 321–338

Nishikawa S-i, Zinkl GM, Swanson RJ, Maruyama D, Preuss D (2005) Callose (β-1, 3 glucan) is essential for *Arabidopsis* pollen wall patterning, but not tube growth. **BMC Plant Biol** 5: 22

Palanivelu R, Brass L, Edlund AF, Preuss D (2003) Pollen tube growth and guidance is regulated by POP2, an *Arabidopsis* gene that controls GABA levels. **Cell** 114: 47–59

Palanivelu R, Preuss D (2000) Pollen tube targeting and axon guidance: Parallels in tip growth mechanisms. **Trends Cell Biol** 10: 517–524

Preuss D (2002) Sexual signaling on a cellular level: Lessons from plant reproduction. **Mol Biol Cell** 13: 1803–1805

Preuss D, Rhee SY, Davis RW (1994) Tetrad analysis possible in *Arabidopsis* with mutation of the *QUARTET* (*QRT*) genes. **Science** 264: 1458–1460

Ray S, Park S-S, Ray A (1997) Pollen tube guidance by the female gametophyte. **Development** 124: 2489–2498

Šamaj J, Müller J, Beck M, Böhm N, Menzel D (2006) Vesicular trafficking, cytoskeleton and signalling in root hairs and pollen tubes. **Trends Plant Sci** 11: 594–600

Shi DQ, Liu J, Xiang YH, Ye D, Sundaresan V, Yang WC (2005) SLOW WALKER1, essential for gametogenesis in *Arabidopsis*, encodes a WD40 protein involved in 18S ribosomal RNA biogenesis. **Plant Cell** 17: 2340–2354

Speakman JR (2013) Functional analysis of seven genes linked to body mass index and adiposity by genome-wide association studies: A review. **Hum Hered** 75: 57–79

Sundaresan V, Springer P, Volpe T, Haward S, Jones JD, Dean C, Ma H, Martienssen R (1995) Patterns of gene action in plant development revealed by enhancer trap and gene trap transposable elements. **Genes Dev** 9: 1797–1810

Wang L, Wang W, Wang YQ, Liu YY, Wang JX, Zhang XQ, Ye D, Chen LQ (2013) *Arabidopsis* galacturonosyltransferase (GAUT) 13 and GAUT14 have redundant functions in pollen tube growth. **Mol Plant** 6: 1131–1148

Wilhelmi LK, Preuss D (1996) Self-sterility in *Arabidopsis* due to defective pollen tube guidance. **Science** 274: 1535–1537

Wilsen KL, Lovy-Wheeler A, Voigt B, Menzel D, Kunkel JG, Hepler PK (2006) Imaging the actin cytoskeleton in growing pollen tubes. **Sex Plant Reprod** 19: 51–62

Xia C, Wang YJ, Li WQ, Chen YR, Deng Y, Zhang XQ, Chen LQ, Ye D (2010) The *Arabidopsis* eukaryotic translation initiation factor 3, subunit F (AteIF3f), is required for pollen germination and embryogenesis. **Plant J** 63: 189–202

Yang KZ, Xia C, Liu XL, Dou XY, Wang W, Chen LQ, Zhang XQ, Xie LF, He L, Ma X (2009) A mutation in *Thermosensitive Male Sterile 1*, encoding a heat shock protein with DnaJ and PDI domains, leads to thermosensitive gametophytic male sterility in *Arabidopsis*. **Plant J** 57: 870–882

Yang WC, Ye D, Xu J, Sundaresan V (1999) The *SPOROCYTELESS* gene of *Arabidopsis* is required for initiation of sporogenesis and encodes a novel nuclear protein. **Genes Dev** 13: 2108–2117

Yu H, Goh CJ (2000) Identification and characterization of three orchid MADS-box genes of the *AP1/AGL9* subfamily during floral transition. **Plant Physiol** 123: 1325–1336

SUPPORTING INFORMATION

Additional supporting information may be found in the online version of this article at the publisher's web-site.

Table S1. Comparison of pollen grains with dotted callose deposition in wild type, mutant and complemented mutant plants

Table S2. The *in vivo* Germination of pollen grains from *attmem18/+* mutant and wild type plants

Table S3. Genetic analyses of progeny from different transgenic *attmem18/+* plants

Table S4. The sequences of primers used in this study

Figure S1. The full length wild type *AtTMEM18* sequence could complement the phenotype of *attmem18* pollen

Figure S2. The structure and location of the fused proteins expressed by the six constructs

Figure S3. Location of p*LAT52:cAtTMEM18-GFP* construct in transgenic pollen grains